

Modelling and Analysis of Voltage Mode Controlled Luo Converter

Divya Navamani Jayachandran, Vijayakumar Krishnaswamy,
Lavanya Anbazhagan and Karthikeyan Dhandapani

Department of EEE, SRM University, India

Article history

Received: 27-08-2014

Revised: 09-04-2015

Accepted: 06-10-2015

Corresponding Author:

Divya Navamani Jayachandran

Department of EEE, SRM

University, India

Email: divyanavamani.j@ktr.srmuniv.ac.in

Abstract: This paper presents the analysis of open loop power stage dynamics relevant to voltage mode control for elementary Luo DC-DC converter for certain specific applications like Hybrid Electric Vehicles, fuel cell vehicles. A comparative analysis is carried out on positive output super lift series of converters to evaluate voltage gain, output voltage ripple, stresses on the switches and efficiency. The most suitable converter is modelled and verified using State Space average method and Circuit averaging technique. The transfer function from duty cycle to output voltage and input voltage to output voltage are derived. The transfer function can be used in modelling the complete Luo converter when voltage mode control is used. Also a simple efficiency modelling technique is proposed with computer simulation using MATLAB/SIMULINK that confirms the predicted results.

Keywords: Luo Converter, Small Signal Transfer Function, Efficiency Modeling, Voltage Mode Control

Introduction

Electrical power systems in future hybrid and fuel cell vehicles may employ three voltage (14V, 42V and High Voltage (HV)) nets. High step up DC-DC converter is necessary for many applications such as FCV, HEV to step up the voltage to high level. One of the key blocks inside hybrid electric vehicles is the DC-DC converter for auxiliary power supply of electric loads. The nominal voltage at the low voltage side of one input is 12 V and can vary from 8 to 16 V during charging and discharging. The nominal high-side voltage is 288 V, with an operating range from 255-425V. Nominal charging and discharging power is 1.5 kW. Switching frequency is 70-100 kHz. Battery power systems often stack cells in series to achieve higher voltage. However, sufficient stacking of cells is not possible in many high voltage applications due to lack of space. Boost converters can increase the voltage and reduce the number of cells. The NHW20 model Toyota Prius HEV uses a 500 V motor. Without a boost converter, the Prius would need nearly 417 cells to power the motor. However, a Prius actually uses only 168 cells and boosts the battery voltage from 202 to 500 V. Further with the use of relift converter, use of 3 batteries is enough to power up to 500V. Voltage Lift (VL) technique is a popular method widely used in electronic circuit design. It has been successfully employed in dc/dc converter applications in recent years and opened a way to design high voltage gain converters.

Four series Luo converters (Luo, 1999a; 1999b; 2000; Luo *et al.*, 2002; Luo and Ye, 2001) are the examples of VL technique implementations.

Dynamic behavior modeling of nonlinear Pulse Width Modulated (PWM) dc-dc converters has been studied in previous literature (Middlebrook and Cuk, 1970; Severns and Bloom, 1985; Polivka *et al.*, 1986; Vorpérian, 1990; Kazimierczuk and Czarkowski, 1993). Modeling of open-loop as well as closed-loop Pulse-Width Modulated (PWM) dc-dc converters is necessary for dynamic and stability analysis of non-linear PWM dc-dc converters. Accurate modelling of the power stage is necessary to determine closed-loop transfer functions.

Modeling Methods

Modeling is the representation of physical behavior by mathematical means. The Simplified models yield physical insight, allow in design system to operate in specified manner. After basic insight has been gained, model can be refined to account for some of the previously neglected phenomenon. The most commonly used modeling methods are: State space averaging: Matrix based approach which gives insight into quantitative nature of basic averaging approximation and Circuit averaging technique: Method based on equivalent circuit manipulations, resulting in a single equivalent linear circuit model of power stage.

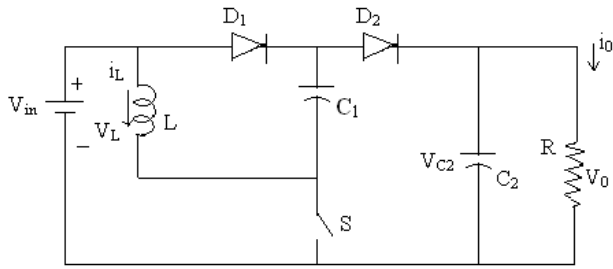


Fig. 1. Elementary Luo converter

The reasons for deriving transfer functions are:

- To analyze the stability and control loop behavior
- To visualize the influence of supply voltage or load changes
- To minimize the influences of supply voltage variations and load changes on the output voltage of a DC/DC converter loop, compensation designs are necessary. The quality of this control circuit design defines the stability of the entire DC/DC converter
- A loop is stable when its phase reaches -180° after the gain has dropped below 1 (= 0dB). If this condition is not fulfilled a frequency exists at which the gain is higher than 1 and the phase shift is exactly 180°
- The impedance measurement could help evaluate possibility of DC/DC converter front-end oscillation
- The duty cycle to output transfer function carries the information needed to determine the structure of the voltage feed- back compensation
- Input to output transfer function is necessary to analyze the audio susceptibility

Modelling of Elementary Luo Converter

Using State Space

Apply KVL Determine A, B, C, E Matrices

Figure 1 shows elementary Luo converter. In this positive output Luo converter, there are two states i.e., when switch is on and when switch is off. During each state we write the following Equation 1 and 2:

$$x' = A_1x + B_1V_d \text{ during } dT_s \quad (1)$$

$$x' = A_2x + B_2V_d \text{ during } (1-d)T_s \quad (2)$$

where, $A_1 + A_2$ are state matrices and B_1 and B_2 are vectors. Let x_1 be inductor current, x_2 represent voltage across capacitor 1, x_3 represent voltage across capacitor 2. Figure 2 and 3 shows the turn on and turn off condition of Luo converter.

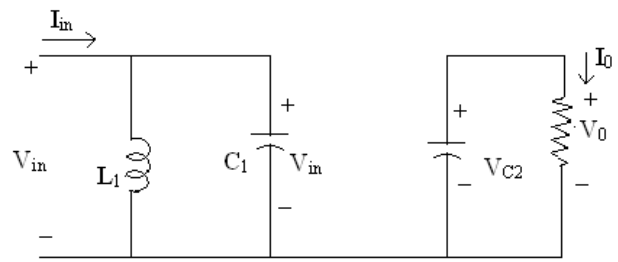


Fig. 2. On state condition

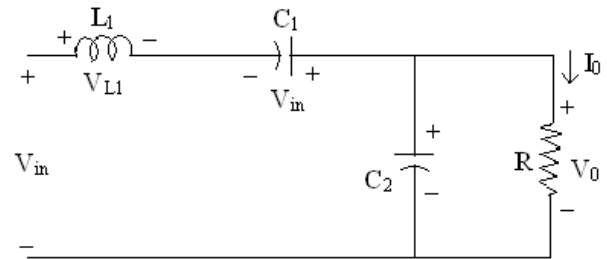


Fig. 3. Off state condition

For turn on:

$$\begin{pmatrix} x_1' \\ x_2' \\ x_3' \end{pmatrix} = \begin{pmatrix} 0 & \frac{1}{L} & 0 \\ -\frac{1}{C_1} & \frac{-1}{(R_1C_1)} & 0 \\ 0 & 0 & \frac{-1}{RC_2} \end{pmatrix} \begin{pmatrix} x_1 \\ x_2 \\ x_3 \end{pmatrix} + \begin{pmatrix} 0 \\ \frac{1}{(R_1C_1)} \\ 0 \end{pmatrix} V_d$$

For turn off:

$$\begin{pmatrix} x_1' \\ x_2' \\ x_3' \end{pmatrix} = \begin{pmatrix} 0 & \frac{1}{L} & \frac{-1}{L} \\ -\frac{1}{C_1} & 0 & 0 \\ \frac{-1}{C_2} & 0 & \frac{-1}{RC_2} \end{pmatrix} \begin{pmatrix} x_1 \\ x_2 \\ x_3 \end{pmatrix} + \begin{pmatrix} \frac{1}{L} \\ 0 \\ 0 \end{pmatrix} V_d$$

$$A = A_1D + A_2(1-D)$$

$$B = B_1D + B_2(1-D)$$

$$A = \begin{pmatrix} 0 & \frac{1}{L} & \frac{-(1-D)}{L} \\ -\frac{1}{C_1} & \frac{-D}{(R_1C_1)} & 0 \\ \frac{(1-D)}{C_2} & 0 & \frac{-1}{RC_2} \end{pmatrix} \quad B = \begin{bmatrix} \frac{(1-D)}{L} \\ \frac{D}{R_1C_1} \\ 0 \end{bmatrix} \quad C = (0 \ 0 \ 1)$$

Using Laplace transformation:

$$S\hat{x}(s) = A\hat{x}(s) + [(A_1 - A_2) \times + (B_1 - B_2)V] \hat{d}(s)$$

$$\hat{x}(s) = [SI - A]^{-1} [(A_1 - A_2) \times + (B_1 - B_2)V] \hat{d}(s)$$

$$\frac{\hat{V}_0(s)}{\hat{d}(s)} = C[SI - A]^{-1} [(A_1 - A_2) \times + (B_1 - B_2)V_d] + (C_1 - C_2)X$$

$$SI - A = \begin{pmatrix} S & \frac{-1}{L} & \frac{(1-D)}{L} \\ \frac{-1}{C_1} & S + \frac{D}{(R_1C_1)} & 0 \\ \frac{-(1-D)}{C_2} & 0 & S + \frac{1}{RC_2} \end{pmatrix}$$

Removing R_i terms:

$$\frac{\hat{V}_0}{\hat{d}} = V_g \left[\frac{-SL \left(\frac{2-D}{(1-D)^2} \right) + R}{S^2 LRC_2 + SL + R(1-D)^2} \right] \quad (3)$$

Circuit Averaging Technique

In ON condition:

$$V_L(t) = V_g(t)$$

$$iC_1(t) = i_g(t) - i(t)$$

$$iC_2(t) = \frac{-V_0}{R}$$

OFF condition:

$$V_L(t) = 2V_g(t) - V_0(t)$$

$$iC_1(t) = i_g(t)$$

$$iC_2(t) = i_g(t) - \frac{V_0}{R} \quad (5)$$

$$V_L(t) = DV_g(t) + D^1(2V_g(t) - V_0(t))$$

$$iC_1(t) = D(i_g(t) \pm i(t)) + D^1(i_g(t)) \quad (6)$$

$$iC_2(t) = D\left(\frac{-V_0}{R}\right) + D^1(i_g(t) - \frac{V_0}{R}) \quad (7)$$

Introducing perturbations:

$$V_g(t) = V_g + \hat{v}_g(t)$$

$$v_0(t) = V_0 + \hat{v}_0(t)$$

$$i_g(t) = I_g + \hat{i}_g(t)$$

$$i(t) = I + \hat{i}(t)$$

Adding perturbations and eliminating DC terms:

$$S\hat{i}(s) = (2-D)\hat{v}_g(s) + \hat{d}(s)[V_0 - V_g] - D^1\hat{v}_0(s)$$

$$C_1S\hat{v}_g(s) = \hat{i}_g(s) - D\hat{i}(s) - \hat{d}(s)I$$

$$C_2S\hat{v}_0(s) = D^1\hat{i}_g(s) - \hat{d}(s)I_g - \frac{\hat{v}_0(s)}{R}$$

We assume $\hat{v}_g(s) = 0$.

Using Dc terms:

$$V_0 = V_g \left(\frac{2-D}{1-D} \right) I_g = \frac{V_0}{RD^1} I = \frac{V_0}{RDD^1}$$

$$\frac{\hat{v}_0(s)}{\hat{d}(s)} = V_g \left[\frac{-SL \left(\frac{2-D}{(1-D)^2} \right) + R}{S^2 LRC_2 + SL + R(1-D)^2} \right] \quad (8)$$

If:

$$C_1 = C_2 = 2 \times 10^{-6}, L = 10 \times 10^{-3}, R = 100\Omega$$

$$\frac{\bar{v}_0(s)}{\bar{d}(s)} = \left[\frac{S(-2.16) + 3600}{S^2(0.000002) + S(0.01) + 25} \right] \quad (9)$$

The transfer functions obtained in the state space averaging and circuit averaging technique are the same and it is shown in the Equation 3 and 8.

Frequency Response Analysis of Luo Converter

A bode plot is a graph of the transfer function of a linear time in variant system versus frequency plotted with a log frequency axis to show the system's frequency response. The transfer function (control to output voltage) obtained from the modeling methods as shown in Equation 9 is used to obtain bode plot, step response and pole zero plot.

The transfer functions derived by state space averaging technique and circuit averging technique are the same. Derived transfer function can be used to determine the stability of the system. It is also used to obtain the closed response of the system. Bode plot drawn from these transfer function shows the operating frequency of the converter and the phase and gain margin tells about the stability of the system.

Figure 4 and 5 shows the step response obtained from the transfer derived. Figure 6 and 7 shows the bode plot for the derived transfer function and their gain margin and phase margin are determined. Figure 8 shows the pole zero plot of the converter. It also shows that the zero lies on the right half of the S-plane. So the system is unstable. A good understanding of the frequency-domain behavior of power converters is achieved.

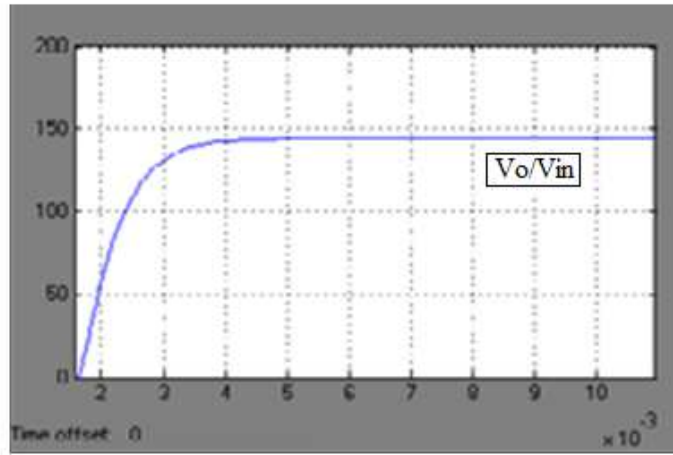


Fig. 4. Step response of input to output transfer function

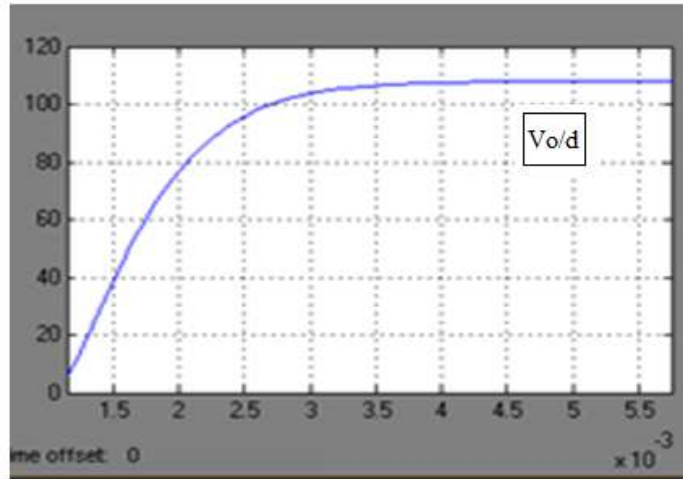


Fig. 5. Step response of duty cycle to output transfer function

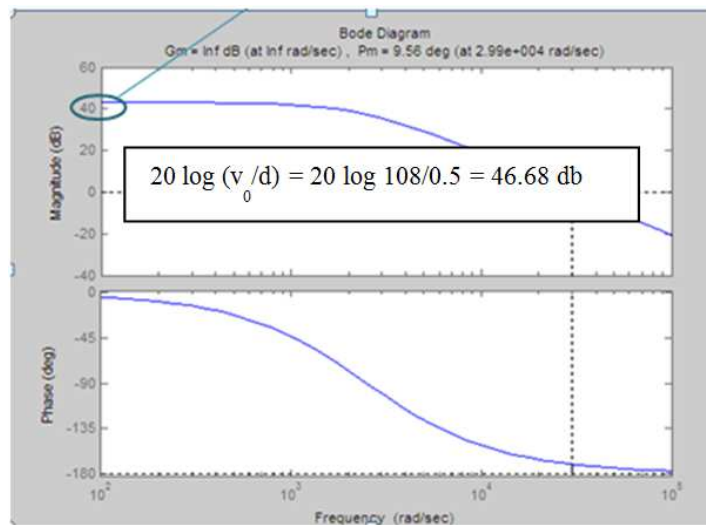


Fig. 6. Bode plot of duty cycle to output transfer function

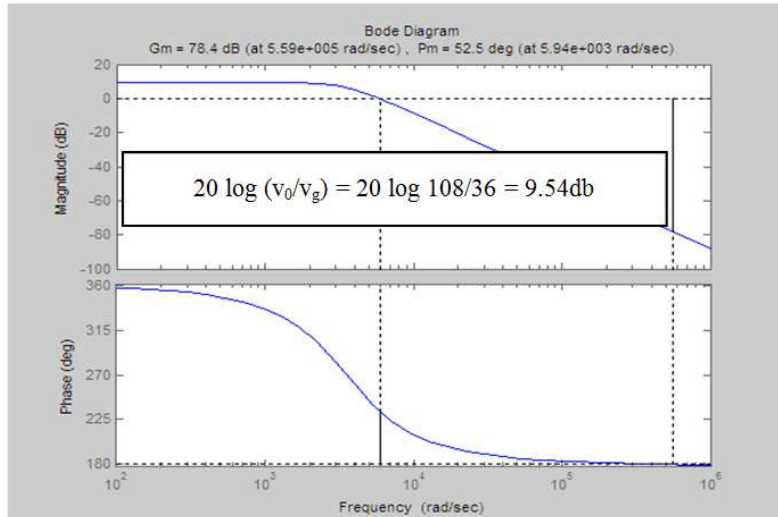


Fig. 7. Bode plot of input to output transfer function

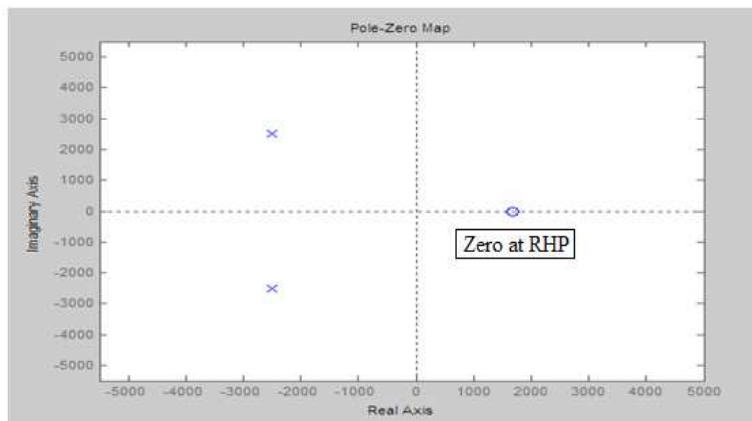


Fig. 8. Pole-zero plot for input to output transfer function

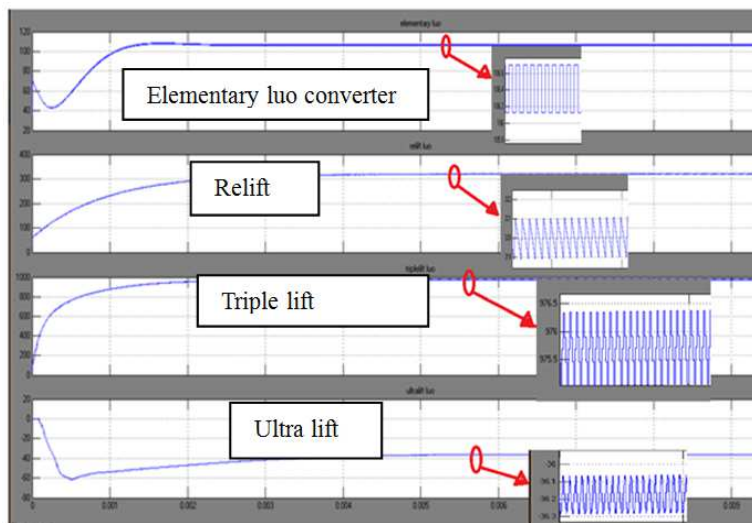


Fig. 9. Simulated output voltage ripple of voltage lift Luo converter

Analysis of Voltage Lift Luo Converter

Different positive super lift converters are compared with the conventional boost converter and their output voltage ripples are analyzed.

Figure 9 shows the simulated output voltage ripple of voltage lift Luo converter. It is found the ripples are very less in elementary luu converter and stresses on the switches are also very less compared to voltage lift luu converter.

Efficiency Model of Elementary Voltage Lift Luo Converter Using Simulink

$$I_{inoff} = I_{I1off} = I_{c1off}$$

$$I_{inon} = I_{I1on} + I_{c1on} \tag{10}$$

$$P_{cond} = I_{out}^2 * R_{DSon} \frac{V_{out}}{V_{in}}$$

$$I_{in} = (2 - k) I_{II} P_{sw} = \frac{CossV^2f}{2} \tag{11}$$

$$\text{Turn on loss} = \frac{(Coss + Cp)V^2f}{2} \tag{12}$$

$$\text{Power loss} = I^2R \quad \text{Efficiency} = \frac{\text{output power}}{\text{output power} + \text{losses}}$$

Equation 10-12 gives conduction and switching losses of the converter. Figure 10 shows efficiency modeling of elementary luu converter with Matlab/simulink. Table 1 gives the comparison between state space averaging and circuit averaging technique. Table 2 gives a brief outlook on different luu converters. Table 3 shows that the efficiency obtained remain same both theoretically and results obtained through modeling.

Voltage Mode Controlled Luo Converter

Designing of PI Controller Using Ziegler-Nichols Tuning Procedure

The Ziegler-Nichols tuning method is performed by setting the *I*(integral) and *D*(derivative) gains to zero. The "P" (proportional) gain, K_p is then increased (from zero) until it reaches the ultimate gain K_u , at which the output of the control loop oscillates with a constant amplitude. K_u and the oscillation period T_u are used to set the P, I and D gains depending on the type of controller used. Using Ziegler Nichols tuning method, the transfer function of the PI controller is:

$$G_p(s) = \frac{0.0000087127s + 0.0099684}{0.000874037s} \tag{13}$$

$$G_p(s).T_f(s) = \frac{-(0.000000706725s^2 + 11.25 + 0.00502875s)}{0.000000002094s^3 + 0.000010471s^2 + 0.0261775s} \tag{14}$$

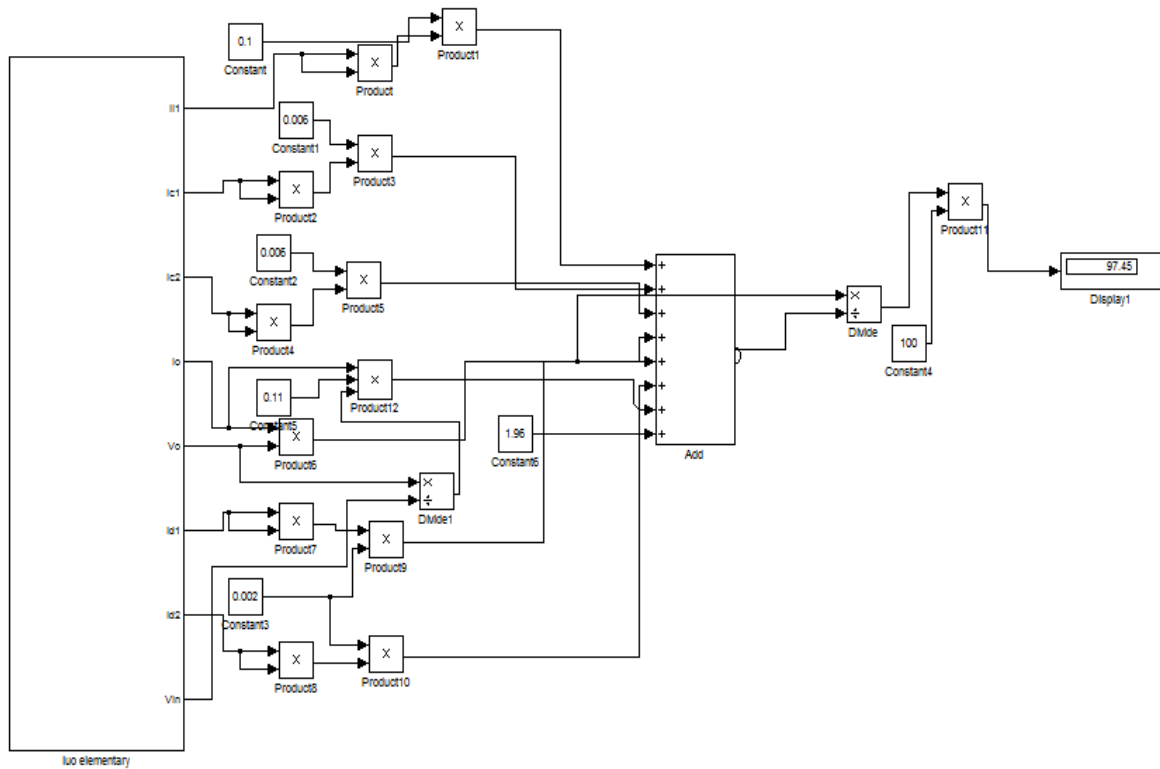


Fig. 10. Efficiency modeling of Elementary luu converter

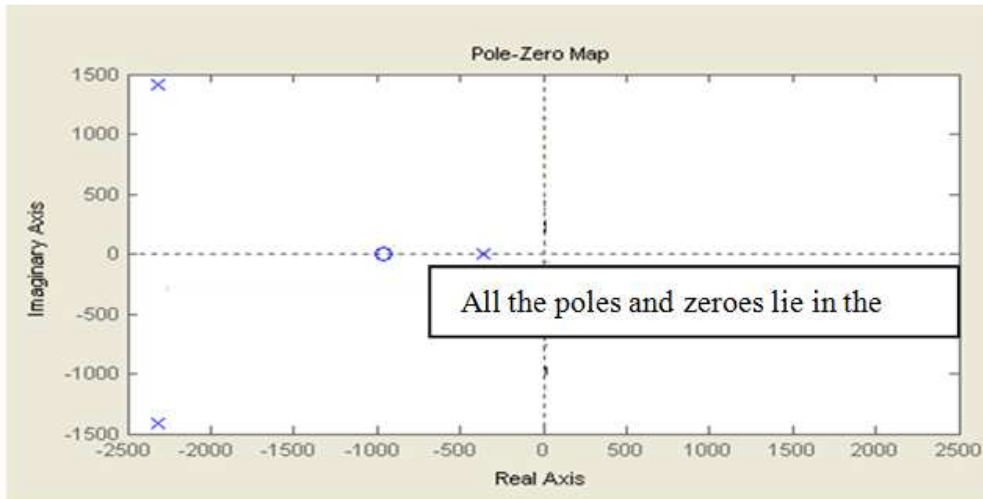


Fig. 11. Plot zero plot-closed loop elementary Luo converter

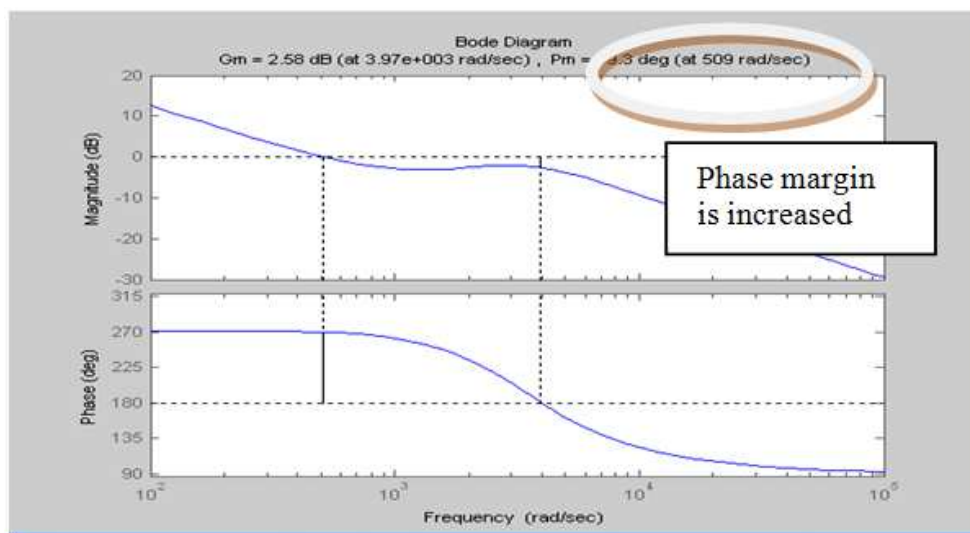


Fig. 12. Bode plot of closed loop Elementary Luo converter

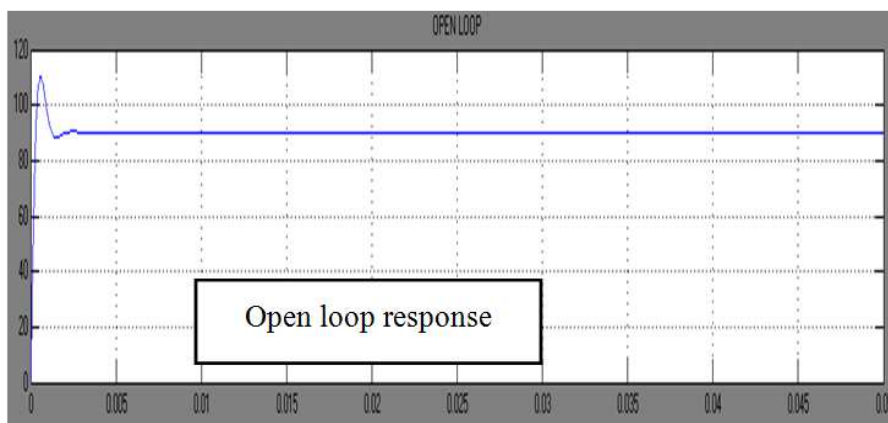


Fig. 13. Open loop response of Elementary Luo converter

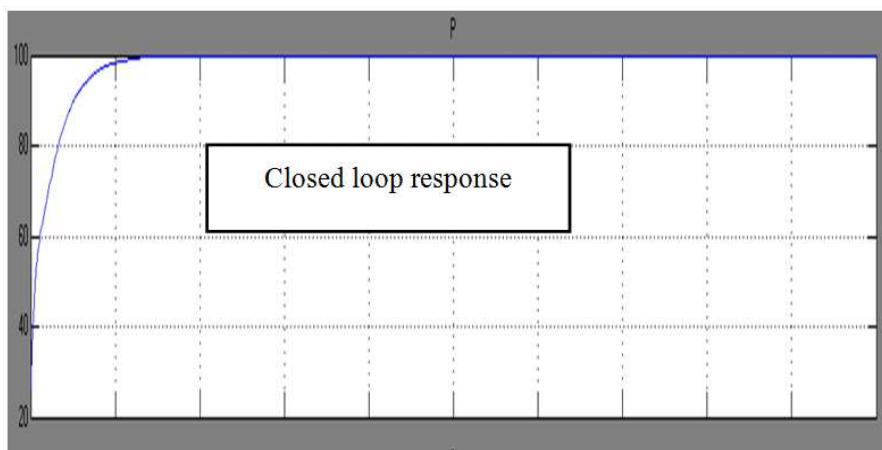


Fig. 14. Closed loop response-tuning the PI controller

Table 1. Comparison between state space averaging and circuit averaging

State space averaging technique	Circuit averaging technique
This approach offers a clear insight into the quantitative nature of basic averaging approximation. This method is tedious when the converter circuit contains a large number of elements. The linearised models, obtained from state-space averaging, do not predict the large-signal stability information and are only sufficient to predict small-signal stability. They are more general and powerful for analyzing and controlling both steady state behavior and small signal perturbations from it.	This approach is using an averaging technique is based on equivalent circuit manipulations, resulting in a single equivalent circuit. Huge approximations for large circuits. Analysis and synthesis can be used in the fullest extent for the design of regulators incorporating switching converters. May not provide complete solution for analyzing and controlling the dynamics of circuits.

Table 2. Comparison of different Luo converter

DC-DC converter	Advantage	Disadvantage
Boost converter	Effective boosting for LCD backlights and flashlights.	Large amount of ripples in output voltage.
Elementary Luo Converter	Cheap topology and high output voltage	Cannot be independently used for very high step up applications like in HEV and smart grid
Superlift Luo Converter	High gains using geometric progressions	Difficult to design because of complexity to resonant circuits
Relift Luo Converter	High power density and high efficiency	Complicated circuit. Circuit becomes bulky.
Ultra Lift Luo Converter	High voltage transfer gain. High output voltage	Cost will be higher compared to relift and elementary Luo Converter
		Negative output voltage. Converter output has to be inverted. Circuitry becomes Large

Table 3. Efficiency comparison

LUO converter	Theoretical efficiency	Simulated efficiency
Elementary Luo converter	98.1%	97.45%

Table 4. Phase margin-luo converter

Parameter	Open loop Luo converter	Closed loop Luo converter
Phase margin	9.56°	89.53°

Equation 13 gives the transfer function of PI controller using Ziegler Nichols second tuning method. Equation 14 gives the closed loop transfer function of elementary loop converter. Figure 11 and 12 shows the pole zero plot and bode plot of the closed loop system.

We can see all the poles and zeroes of the transfer functions are lying on the left half of the s plane. As a result of this, the converter is stable. Also, from the bode plot of the closed loop transfer function we can see that, the phase margin has been raised to high positive value. Also, the gain margin is positive which indicates the stability of the converter under closed loop control. Thus the controller's characteristics provide increased phase margin and improved stability to a DC-DC converter. Table 4 shows the improvement in phase margin from open loop to closed loop system.

As, from the pole zero plot, we can see all the poles and zeroes of the transfer function are lying on the left half of the s plane the converter is stable. Also, from the bode plot of the closed loop transfer function we can see

that, the phase margin has been raised from negative to a marginally high positive value. Also, the gain margin is positive which indicates the stability of the converter under closed loop control.

Figure 13 and 14 shows the response obtained from the open loop and closed loop system. Overshoot in the open loop response is suppressed with the help of PI controller in the closed loop system.

Conclusion

With the increasing demand of renewable energy sources, we have proposed superlift series of Luo converter instead of boost converter, which is typically used in hybrid electric vehicle. For choosing the best converter out of the super lift series of Luo converter, voltage ripple analysis, stress on switches of the converter and efficiency modeling were done on elementary Luo converter, relift Luo converter and triple lift Luo converter. For our application of hybrid electric vehicle, we found elementary Luo converter to be highly suitable.

Modeling of elementary Luo converter has been done using state space averaging method and circuit averaging technique. Using the transfer function obtained, bode plot was drawn for input to output voltage transfer function as well as duty cycle to output voltage transfer function. The poles and zeroes obtained for the transfer function are in the right half of the S plane as compared to buck converter which has zeroes in the left half of the S plane.

Based on the frequency response analysis, the phase margin obtained is very low (2.53 deg) and the gain margin is infinity (inf) which shows that the system is unstable. So we propose to design a closed loop control for the Luo converter in order to make the system stable. A PI controller was designed using Ziegler Nichols tuning method. The PI controller was cascaded with the open loop transfer function obtained from circuit averaging technique as well as state space averaging technique. A closed loop was designed after cascading. The poles and zeroes of the transfer function lie on the left half of the s plane which shows the stability of the closed loop control of the converter, also the phase margin has been raised to 89.3 deg and the gain margin is also positive. All these results prove that the closed loop control of the elementary Luo converter is stable.

Funding Information

The authors have no support or funding to report.

Author's Contributions

Divya Navamani Jayachandran: Actively participated in modelling of Luo converter and closed loop analysis.

Vijayakumar Krishnaswamy: Contributed to the writing of the manuscript.

Lavanya Anbazhagan: Participated in simulating the converter in MATLAB/Simulink and analysing the same.

Karthikeyan Dhandapani: Contributed in frequency response analysis of Luo converter.

Ethics

This article is original and contains unpublished material. The corresponding author confirms that all of the other authors have read and approved the manuscript and no ethical issues involved.

References

- Kazmierczuk, M.K. and D. Czarkowski, 1993. Application of the principle of energy conservation to modeling the PWM converters. Proceedings of the 2nd IEEE Conference on Control Applications, Sep. 13-16, IEEE Xplore Press, Vancouver, BC, pp: 291-296. DOI: 10.1109/CCA.1993.348274
- Luo, F.L. and H. Ye, 2001. DC/DC conversion techniques and nine series Luoconverters. In: Power Electronics Handbook, Rashid, M.H. (Ed.), CA, Academic, San Diego, pp: 17-17.
- Luo, F.L., 1999a. Negative output Luo converters: Voltage lift technique. Proc. Inst. Elect. Eng., 146: 208-224. DOI: 10.1049/ip-epa:19990302
- Luo, F.L., 1999b. Positive output Luo converters: Voltage lift technique. Proc. Inst. Elect. Eng., 146: 415-432. DOI: 10.1049/ip-epa:19990291
- Luo, F.L., 2000. Double-output Luo converters, an advanced voltage-lift technique. Proc. Inst. Elect. Eng., 147: 469-485. DOI: 10.1049/ip-epa:20000622
- Luo, F.L., H. Ye and M.H. Rashid, 2002. Multiple-quadrant Luo-converters. Proc. Inst. Elect. Eng., 148: 9-18. DOI: 10.1049/ip-epa:20020024
- Middlebrook, R.D. and S. Cuk, 1970. A general unified approach to modelling switching-converter power stages. Proceedings of the Power Electronics Specialists Conference, Jun. 8-10, IEEE Xplore Press, Cleveland, OH, pp: 18-34. DOI: 10.1109/PESC.1976.7072895
- Polivka, W.M., P.R.K. Chetty and R.D. Middlebrook, 1986. State-space average modeling of converters with parasitics and storage time modulation. Proceedings of the Power Electronics Specialists Conference, (ESC' 86), pp: 119-143.
- Severns, R.P. and G. Bloom, 1985. Modern DC-to-DC Switchmode Power Converter Circuits. 1st Edn., Springer Netherlands, Springer, ISBN-10: 9401180873, pp: 30-42.
- Vorpérian, V., 1990. Simplified analysis of PWM converters using model of PWM switch. Continuous conduction mode. IEEE Trans. Aerosp. Electron. Syst., 26: 490-496. DOI: 10.1109/7.106126